JES Focus Issue of Selected Papers from IMLB 2018

Aqueous Binder for Nanostructured Carbon Anode Materials for Li-Ion Batteries

Marcelina Lis,[1] Krystian Chudzik,[1] Monika Bakierska,[1] Michał Świętosławski,[1] Marta Gajewska,[2] Małgorzata Rutkowska,[1] and Marcin Molenda [1,z]

[1] *Jagiellonian University, Faculty of Chemistry, 30-387 Krakow, Poland*
[2] *AGH University of Science and Technology, Academic Centre for Materials and Nanotechnology, 30-059 Krakow, Poland*

Water soluble hydrophilic polymer poly-N-vinylformamide (PNVF) has been adopted as new binder for selected anode materials based on nanostructured carbon aerogels (CAGs) derived from different types of starch (rice, maize, potato) as well as for graphite as a reference. The results suggest that PNVF can be promising, fluorine free and volatile organic compounds (VOC) free binder for some anode materials especially when taking into consideration its beneficial properties, cost reduction as well as environmental friendliness. PNVF enhances chemical and physical interactions with tested carbons improving adhesion strength of the created composites and thus capacity retention of the formed electrodes during extensive cycling under high current load. Herein, we show that although the binder is only a small part of the entire electrode composition, it has a huge impact on the properties and efficiency of lithium-ion battery. Thereby, every anode material require properly selected binder for the suitable operation and performance of the cell.

 [DOI: 10.1149/2.0591903jes]

Manuscript submitted October 29, 2018; revised manuscript received January 7, 2019. Published January 18, 2019. *This paper is part of the JES Focus Issue of Selected Papers from IMLB 2018.*

One of the most significant challenges facing the modern world of science is to provide reliable and efficient energy storage systems for ever-evolving industry. Nowadays the major role in this field is played by Li-ion batteries. However, there is still a need for dynamic progress in improving the operation parameters of the cells, hence even this popular Li-ion technology is constantly optimized.[1,2] One of the key issues to meet the expectations of industry in accomplishing Li-ion batteries is a properly designed electrode. It is commonly known that apart from active materials, the integral parts of electrode are conductive additives and binders. The latter one is crucial for the integrity to form the electrode with suitable mechanical and electrical properties.[3–5]

Binders need to exhibit good adhesion to electrode materials and current collectors, high electrochemical stability over a wide range of potentials, high melting point and should not limit ionic and electronic conductivity.[6–8] The most popular one is poly(vinylidene difluoride) (PVDF). Nevertheless, despite good binding properties it has to be noticed that PVDF has the tendency to swell in ionic liquids. Moreover, PVDF needs to be dissolved in an organic diluent such as N-methyl-2-pyrrolidone (NMP) to fabricate a proper slurry. Thus, using NMP is directly connected with negative environmental impact as well as higher cost of electrode production and Li-ion batteries recycling due to fluorine content.[9–13] Therefore, mainly for these issues there is a necessity for developing new, water soluble binders for Li-ion batteries.

There is no doubt, that organic solvent free binders have been widely explored in recent years.[2,6,12–16] Among them, the sodium carboxymethyl cellulose (CMC),[2,13,15–18] poly(acrylic acid) (PAA) and its modification (PAAX, X = Li, Na, K, NH_4),[17–20] styrene butadiene rubber (SBR),[14,18] poly(vinyl alcohol) (PVA),[9,15] polyacrylonitrile (PAN)[21] etc. are intensively studied to make the electrode processing non-hazardous for nature and less expensive. Furthermore, the alternative binders for lithium-ion batteries are already available on the worldwide market which also underlines the significance of their progress.[13]

On the other hand, there is also need to remember that for the suitable operation of the cell, every electrode material require properly selected binder. Hence, in this work we propose the application of water-soluble, hydrophilic polymer poly-N-vinylformamide as electrode binder, especially suitable for functionalized carbonaceous anodes. As recent reports show, there are also attempts to apply PNVF for cathode material ($LiFePO_4$).[22] During our studies the binding potential of PNVF for the graphitic anode as well as for the novel, bio-derived, nanostructured carbon aerogels based anodes[23–25] was investigated. Our aerogels are explored as a potential, renewable alternatives for natural or artificial (from fossil fuels) graphite to support the global energy sustainability with the lowest carbon footprint. These research aimed to improve the performance of the carbon electrodes for their better operation along with the cost reduction and the natural habitat protection.

Experimental

The poly-N-vinylformamide was obtained by free radical polymerization of N-vinylformamide (NVF) in aqueous solution at 60°C under the constant flow of argon. As an initiator 2,2'-Azobis(2-methylpropionamidine) dihydrochloride (AIBA) was added in molar ratio 1:100 initiator to monomer. The PNVF was dried in air at 90°C for 24 h.

The PVDF powder (Sigma Aldrich, M_w∼534000 by GPC) was used as a reference binder.

The crystallinity of the polymers was analyzed by X-ray powder diffraction (XRD) using BRUKER D2 PHASER diffractometer with Cu $K_{\alpha 1}$ radiation, $\lambda = 0.154184$ nm. Using Shimadzu chromatograph with PolySep-GFC-P 3000 column (GPC) the average molecular weight of PNVF was determined. The thermal stability of the binders in contact with liquid electrolyte was investigated by DSC measurements that were performed on 821^e Mettler-Toledo equipment in the temperature range from 25 to 400°C, under constant flow of argon with a heating rate equal to 10°C/min. In order to investigate the electrochemical stability of PNVF binder the cyclic voltammetry measurements (CV) were conducted on the potentiostat/galvanostat PGSTAT302N/FRA2 (AUTOLAB) in the potential range of 0–3 V (vs. Li/Li^+) at scan rate of 0.01 mV/s. As the working electrode a copper foil was coated with a thin polymer film and as the electrolyte 1M $LiPF_6$ in a mixed-solvents of ethylene carbonate and diethyl carbonate EC/DEC (50/50 v/v, Sigma-Aldrich, battery grade) was applied.

[z] E-mail: molendam@chemia.uj.edu.pl

The effect of polymer binders on the cycling performance of the electrodes based on graphite (MTI, battery grade) as well as on carbon aerogels obtained from rice (RS), maize (MS) and potato (PS) starches was examined by galvanostatic charge discharge test (GCDT) vs. Li/Li^+ between 0.001 and 3.0 V at different current rates using R2032 coin-type cells. The preparation process of CAG materials was presented in our previous work.[23–25] The cell tests were carried out using the ATLAS 0961 MBI multichannel battery tester (ATLAS-SOLLICH). The anode electrodes were prepared by mixing 90 wt% of active material with 10 wt% of PVDF or PNVF in NMP (Sigma Aldrich, ≤99,5%) or distilled water, respectively. The slurry was coated on copper current collector. The cells were assembled in an argon-filled glove box (MBraun glove box) with both H_2O and O_2 levels less than 0.1 ppm. As separators a trilaminate of polypropylene/polyethylene/polypropylene film (Celgard 2325) and two porous glass microfiber filters (Whatman GF/F) were used. The applied electrolyte was the same as mentioned before. To investigate the morphology of the CAG based electrodes before and after the electrochemical performance, an FEI Versa 3D (FEG) scanning electron microscope (SEM) was utilized. Additionally, the morphology of investigated binders was also examined.

Carbon aerogels and graphite were characterized in terms of their morphology. The X-ray photoelectron spectra (XPS) of the carbonaceous materials were measured on a Prevac photoelectron spectrometer equipped with a hemispherical VG SCIENTA R3000 analyzer. XPS experiments were taken with a monochromatized aluminum source Al K_α (E = 1486.6 eV) and a low energy electron flood gun (FS40A-PS) to compensate charge on the surface during measurements. Peaks were recorded with a constant pass energy of 100 eV for the survey and high resolution spectra. Binding energies were referenced to the gold (84.0 eV). Fitting of the high resolution spectra was provided through the CasaXPS software. Textural properties of the samples were determined by N_2-sorption at -196°C using a 3Flex v1.00 (Micromeritics) automated gas adsorption system. Prior to the analysis, the samples were degassed under vacuum at 350°C for 24 h. The specific surface area (S_{BET}) of the samples was determined using the Braunauer-Emmett-Teller (BET) model. The external surface area and the micropores volume were calculated from the *t*-plot model using the Carbon Black STSA thickness curve.

Results

Firstly, the crystal structures of binders as well as their thermal and electrochemical stabilities were examined. Fig. 1a presents XRD diffraction patterns as well as SEM images of pristine PNVF (M_w∼70000 by GPC) and PVDF powders. It is observed that PVDF is a semi-crystalline and has more regular shape (small globules accumulated together) while PNVF is amorphous and composed of disordered particles. These differences can have a great impact on the morphology of polymer films that are formed during anode preparation process as well as on their binding abilities.[15,17]

The results of DSC experiments are illustrated in Figs. 1b–1c. In Fig. 1b it can be seen that PNVF powder exhibits strong endothermic effect in the range of 230–270°C that is connected with the polymer degradation.[26] This strong endothermic effect can be potentially used to absorb heat released in case of exothermic cell failure, thus increase cell safety. In Fig. 1c DSC curves for used electrolyte and polymer (PNVF as well as PVDF) suspensions are displayed. Strong endothermal peak connected with solvent/salt decay in electrolyte is shifted after the addition of the binders. For pure electrolyte sample the peak is located in 220–290°C range- PVDF changes the decomposition temperature range slightly (215–285°C) while PNVF lowers it remarkably to 165–225°C range. Nonetheless, all these temperatures are far above typical working conditions of the Li-ion cell. Broad endothermic peak in 100–160°C range is attributed to loss of remaining water from the PNVF binder. A peak connected with decomposition of the PNVF is moved insignificantly toward lower temperatures when it is compared to DSC curve of the polymer powder. The electrochemical stability of the PNVF was introduced in Fig. 1d. There are no additional peaks resulted from the inherence of the polymer on the CV curves what shows that PNVF is fully stable as a binder in the potential range 0–3 V.

Galvanostatic charge-discharge tests were performed to investigate the effect of polymer binders on the cycling performance of the studied anode materials i.e. graphite and novel, nanostructured carbons (CAG_PS, CAG_MS, CAG_RS). Fig. 2 shows voltage curves for the 1st and 400th cycles of the CAGs electrodes and graphite with two different binder materials used in electrodes fabrication (PVDF – Fig. 2a and PNVF – Fig. 2b) at a current rate of 5C (C-rate is defined as a current which is needed to fully charge/discharge the battery in a specific time, e.g. 1C is a current required to fully charge/discharge the cell within 1 hour). In case of long-term cycling, the loading level of each electrode was about 1.07 mg/cm^2 for electrodes with PNVF binder as well as 1.20 mg/cm^2 for electrodes with PVDF one. The presented voltage profiles of the prepared carbon aerogels reveal the typical electrochemical behavior of disordered carbons with graphene domains, sharing some common traits, such as noticeable charge and discharge voltage hysteresis, high irreversible capacity and indistinguishable plateaus. The large loss in the initial capacity of all cells can be attributed to the electrolyte decomposition and the subsequent formation of solid electrolyte interface (SEI) layer on the electrode surface. Nevertheless, it should be pointed out that the irreversible capacity practically disappears after the initial electrochemical processes, indicating high stability and reversibility of examined systems what is reflected in Fig. 3. Together with the increase in the coulombic efficiency for all studied samples at the beginning of the electrochemical cycling, we can observe the gradual increase of the specific capacity that can be attributed to the activating process of initially unexposed pores in carbon electrodes. The highest values of specific capacity from entire group of tested electrode materials are delivered by the cells containing CAG_PS (PNVF) (Fig. 3a), CAG_MS (PVDF) (Fig. 3b), CAG_RS (PVDF) and CAG_RS (PNVF) (Fig. 3c) electrodes and after 400 cycles were still maintained at 206, 207, 205 and 205 mAh/g in the given order Remarkably lower charge capacities were achieved for graphite electrode - 88 and 40 mAh/g after 400 cycles in reference to PVDF and PNVF binders (Fig. 3d). Considering these results, we should draw attention to the fact, that the use of PNVF binder leads to the great capacity improvement of CAG_PS sample compared to the same carbon aerogel in conjunction with PVDF binder. On the contrary, such beneficial effect of PNVF binder is not visible for CAG_MS material and graphite, which in this combination exhibit lower capacities. An interesting case concerns CAG_RS, for which the role of utilized binder is less significant as both CAG_RS (PVDF) and CAG_RS (PNVF) electrodes operate at the comparable level and hence demonstrate similar working parameters in terms of electrochemical processes capacity. Moreover, Fig. 4 shows the results of multiple-step galvanostatic cell tests, carried out using different current rates (from 1C to 50C and then back to 1C), after 10 cycles of preliminary activation process under C/2 current rate. For these tests, the typical mass loading of active material in electrodes was established to about 1.35 mg/cm^2 and 1.53 mg/cm^2 for PNVF and PVDF based electrodes, respectively. As it can be observed, the discharge and charge capacities decreased with the increase of current rate for all cells, but when the current rate was set back to 1C, the specific capacities recovered approximately to initial values, confirming that rapid electrochemical lithiation/delithiation (at 50C) do not cause any permanent damage to the structure and SEI of carbon aerogels and graphite. The highest achieved charge capacities of 372 and 328 mAh/g were delivered under 1C rate by the cells including CAG_PS (PNVF) (Fig. 4a) and graphite (PVDF) (Fig. 4d) electrodes. Despite this favorable feature of graphite sample, its electrochemical characteristics in terms of rate capability is not satisfactory as the rise of the current rate to 5C contributed to huge capacity deterioration. In this matter CAG materials unveil much better behavior. Further, the given electrochemical characteristics of the prepared carbon aerogels are in good accordance with the presented above results of long-term charge/discharge tests (Figs. 3a–3c). Both CAG_MS (Fig. 4b) and CAG_RS (Fig. 4c) electrodes show greater performance with the use

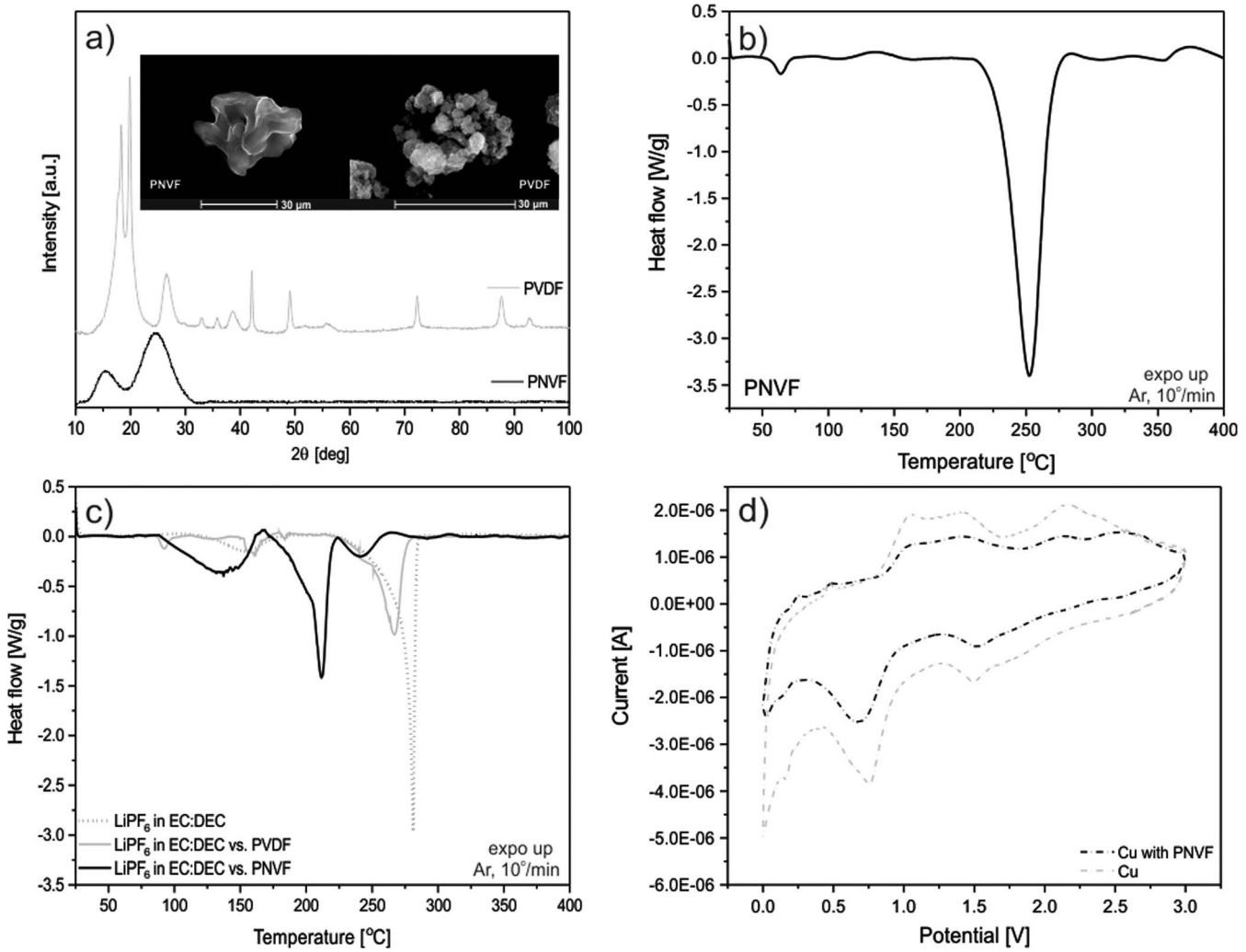

Figure 1. a) X-ray diffraction patterns as well as scanning electron microscopy micrographs of the PNVF and PVDF binders, b) Differential scanning calorimetry results of PNVF, c) DSC curves of the pure $LiPF_6$ in EC:DEC electrolyte solution and the results of its stability toward PVDF and PNVF polymers, d) Cyclic voltammetry of PNVF binder.

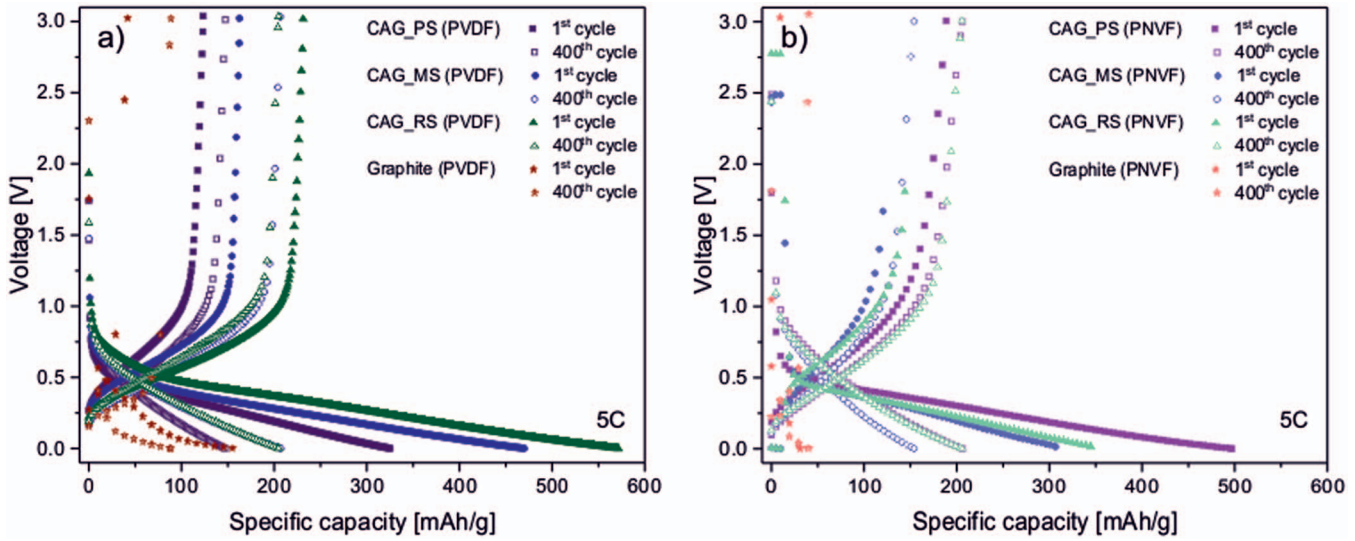

Figure 2. Charge-discharge voltage profiles for the 1st and 400th cycle of CAG_PS, CAG_MS, CAG_RS, graphite based electrodes with a) PVDF binder b) PNVF binder at 5C current rate.

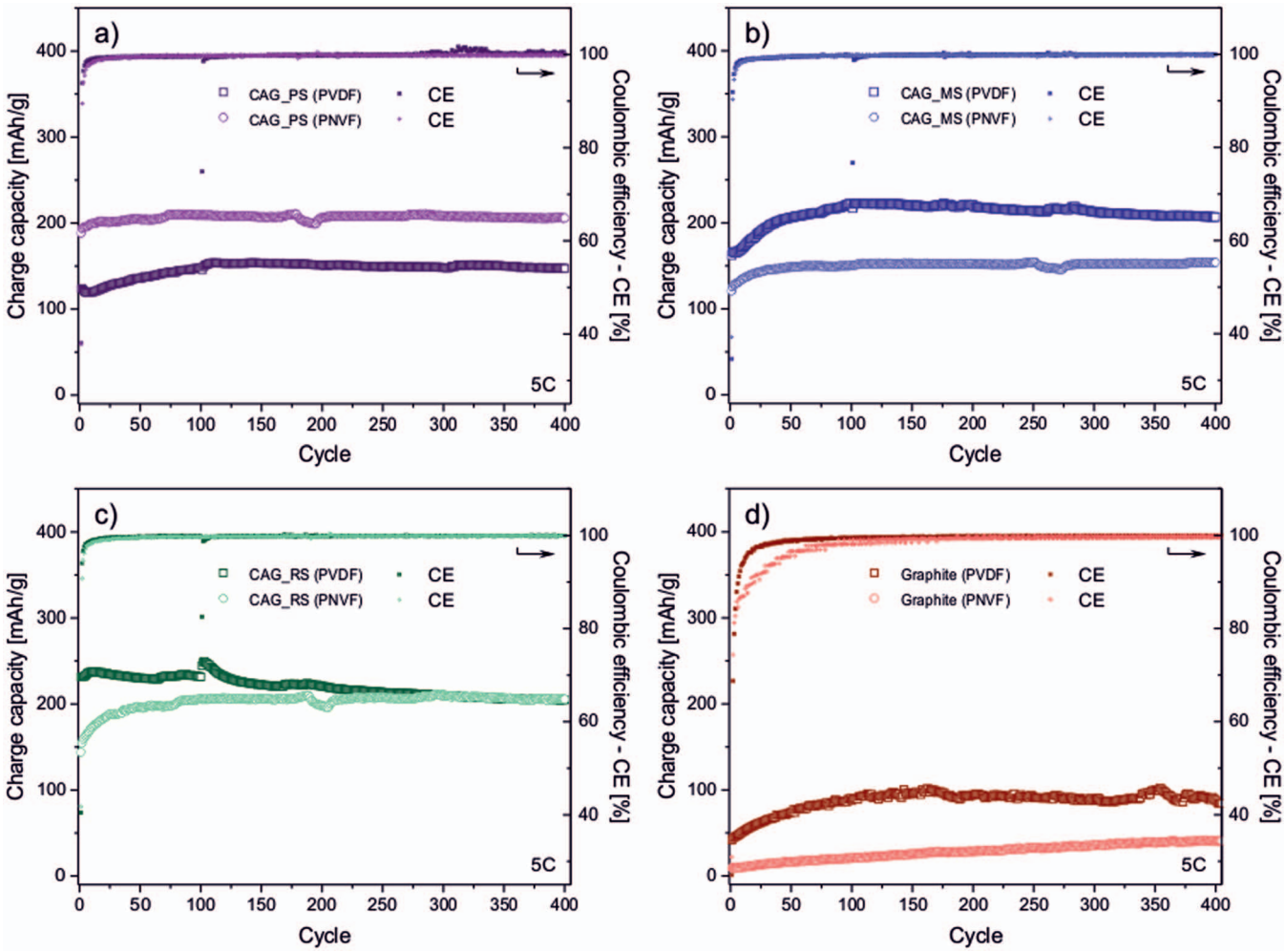

Figure 3. Long-term cycling performance at 5C of a) CAG_PS, b) CAG_MS, c) CAG_RS, d) graphite electrodes.

of PVDF binder. On the other hand, it should be specified that in case of CAG_RS material, the influence of binder on the operation parameters is less apparent under higher current densities.

For better electrochemical characteristics of investigated systems the impedance spectroscopy (EIS) measurements were carried out (Figs. 5a–5d). As it can be seen the Nyquist plots are consisted of three parts – two depressed semicircles (the first at the high-frequency region and the second at the mid-frequency region) and the straight line at the low frequency region. These parts of the spectra can be interpreted in the following way: R_1 corresponds to uncompensated ohmic resistance which is the result of electrolyte resistance and electrical contact between active material and current collector, R_{SEI}/CPE_1 is assigned to the SEI layer formation (high-frequency semicircle), R_{CT}/CPE_2 is associated with the charge-transfer process (mid-frequency semicircle) and CPE_3 is related to the bulk Li^+ diffusion (low-frequency straight line). As it was calculated graphite exhibits drop in R_{CT} values after cycling (from 22 Ω to 16.7 Ω) and in R_{SEI} values (from 7.2 Ω to 5.3 Ω) when the binders were switched from PVDF to PNVF, respectively (Fig. 5d). These changes are also reflected in long-term galvanostatic charge-discharge tests. CAG-based electrodes exhibit similar behavior after the binder alteration. The changes in R_{CT} value for all CAGs materials when switching binders from PVDF to PNVF are noticeable (Figs. 5a–5c). The R_{CT} values after cycling are equal to 8.9 Ω (CAG_PS), 9.9 Ω (CAG_MS), 9.1 Ω (CAG_RS) for electrodes with PNVF as well as to 16.5 Ω (CAG_PS), 11.0 Ω (CAG_MS) and 14.7 Ω (CAG_RS) as PVDF binder was applied. The highest R_{CT} for CAG_PS with PVDF binder can clarify its worst performance in GCDT measurements. Moreover, these differences can explain significant improvement in rate capability of all carbon based anodes during extensive cycling. A decrease in the charge transfer resistance can be also assigned to enhancing the electrolyte permeation and electrical conductivity after numbers of cycles.

The surface morphology of the CAG electrodes before electrochemical cycling and after 400 cycles of galvanostatic charging/discharging was investigated using SEM. The representative micrographs are illustrated in Fig. 6. In fact, no signs of physical damage are visible on the surface of the CAG based electrodes after the electrochemical reaction as no cracks or separate phases can be distinguished. Observably, the morphology of the cycled electrodes is very similar to that of the fresh electrodes. Hence, we can assert that the prepared carbon aerogels with both utilized binders are stable regarding used electrolyte and adapted conditions of cycling. Nevertheless, it is worth to notice that the individual components that constitute the electrodes (before and after cycling) seem to be better bonded to each other when PNVF binder material is employed in electrodes fabrication.

In order to explain unusual behavior of CAGs and graphite based electrodes with different binders, the investigated materials were studied using the X-ray photoelectron spectroscopy and N_2 sorption method. The recorded XPS C1s and O1s spectra of obtained carbon aerogels as well as studied graphite are quite alike (Fig. 7). There is no implication of large differences of the carbons surfaces. Spectra of all samples consist mainly of the large peak at 284.7 eV which can be assigned to C-C bonding. Weak peaks representing surface groups (ether ~285.8 eV and ester ~287.2 eV) can be observe on

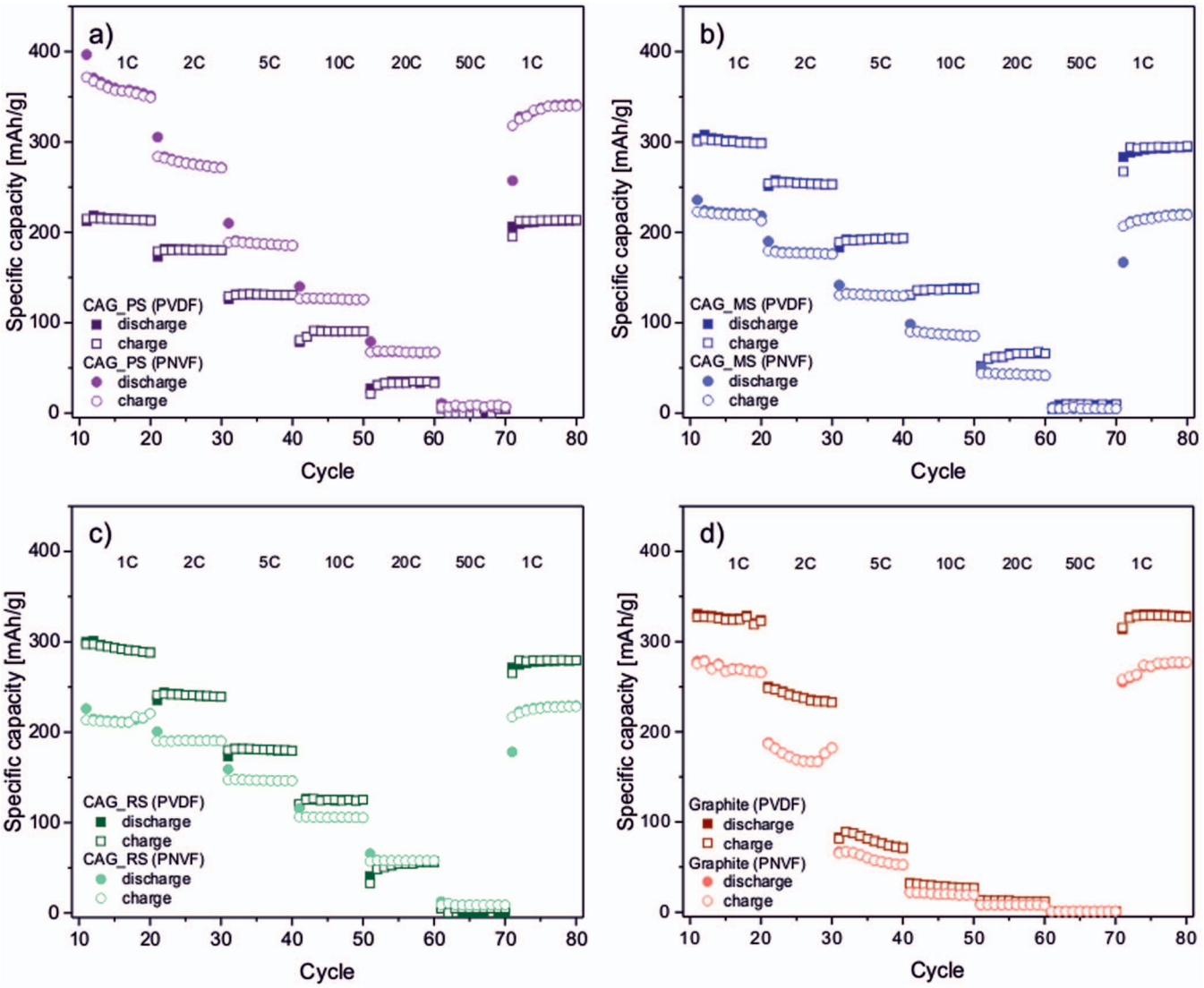

Figure 4. Specific capacity as a function of cycle number for a) Li/Li$^+$/CAG_PS, b) Li/Li$^+$/CAG_MS, c) Li/Li$^+$/CAG_RS, d) Li/Li$^+$/graphite at various C rates.

the bottom of C-C peak. The broad π-π^* satellite from graphite-like domain at around 290–291 eV is visible for all samples. The textural parameters of the samples are presented in Table I. In comparison to graphite, carbon aerogels obtained from the starches are characterized by strongly developed surface parameters, such as BET surface area, external surface area, the volume of micropores and the total pore volumes. Among the bio-derived samples, the following order of the tendency to create highly developed surface was received: maize > rice > potato. It is worth to notice that the textural parameters of CAG_MS and CAG_RS are quite similar, while in case of carbon aerogel obtained from the potato starch the values of S_{BET}, S_{EXT}, V_{MIC} and V_{TOT} are significantly lower. It suggests that CAG_PS may possess less micropores in the structure in comparison to the rest of carbonaceous samples.

Table I. Textural parameters of carbon aerogels based on different types of starches and the reference sample, graphite.

Sample code	S_{BET} [m^2/g]	S_{EXT} [m^2/g]	V_{MIC} [cm^3/g]	V_{TOT} ($p/p_0 = 0.99$) [cm^3/g]
graphite	14	15	—	0.030
CAG_PS	302	73	0.116	0.187
CAG_MS	549	167	0.152	0.310
CAG_RS	520	143	0.149	0.276

Discussion

Displayed outcomes support the statement that the application of PNVF polymer binder outstandingly promotes the electrochemical properties of CAG_PS based electrode and the cycling performance of all selected anode materials. The results suggest that the differences in the electrochemical properties of investigated carbons arise from the diversity in their morphology as well as from the chemical character of applied binders. For all cases the better cycling retention with PNVF binder after long-term charge/discharge tests can be related with the strong binding ability of water-based polymer. Amide groups in PNVF binder interact with available functional groups on the surface of anode materials not only via permanent dipole-dipole interplay but especially via stronger hydrogen bonds. These hydrogen bonds significantly enhanced the adhesion strength of the obtained composites. Thereby, for all cells with PNVF binder the stability (in case of CAG_PS and CAG_MS) or substantial improvement (for CAG_RS and graphite) of specific capacity over cycling are observed. On the other hand, after extensive testing of cells with PVDF it can be seen that the lower adhesion strength (van der Waals interaction between

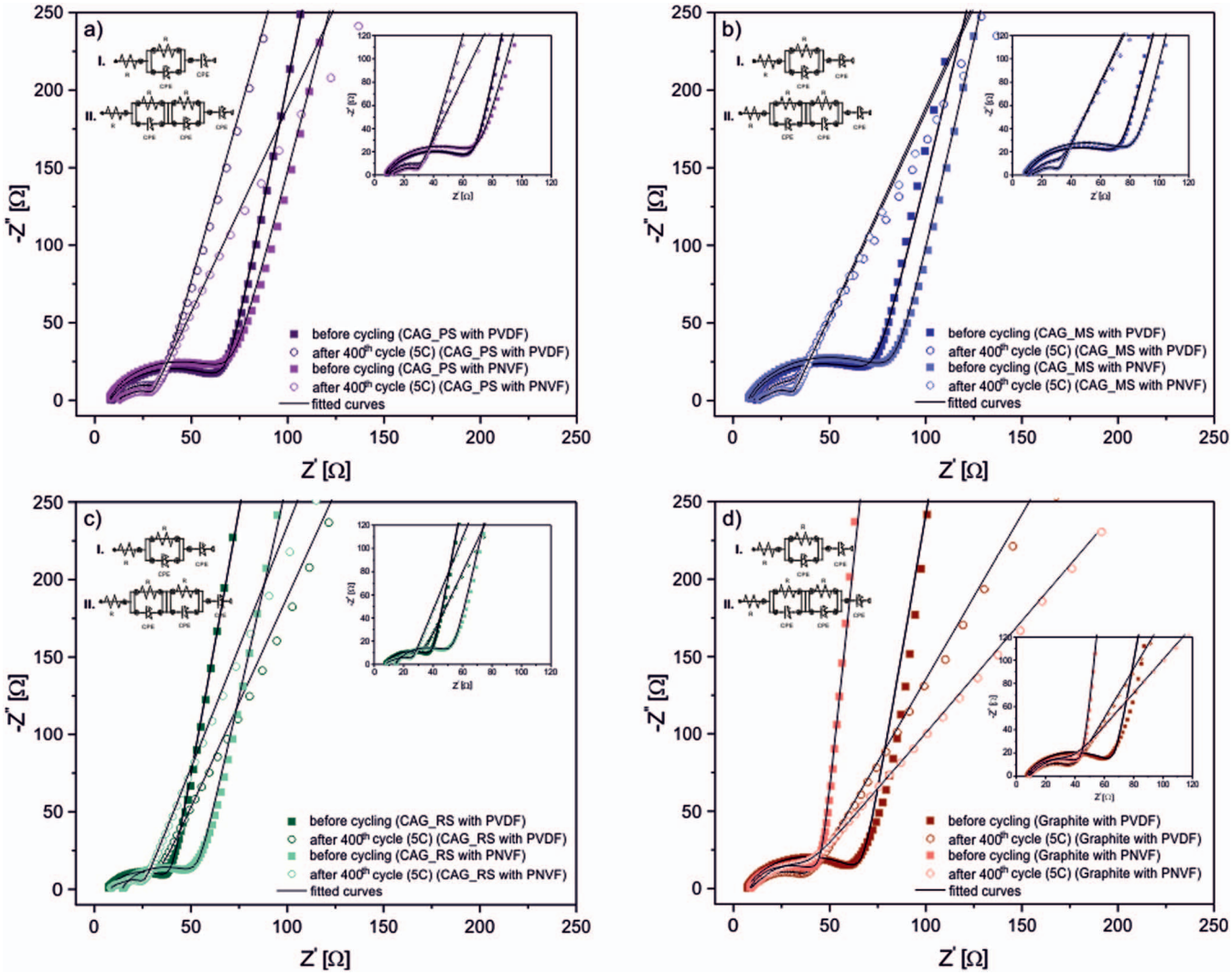

Figure 5. Nyquist plots for a) Li/Li$^+$/CAG_PS, b) Li/Li$^+$/CAG_MS, c) Li/Li$^+$/CAG_RS, d) Li/Li$^+$/graphite cells with the modeled equivalent circuits.

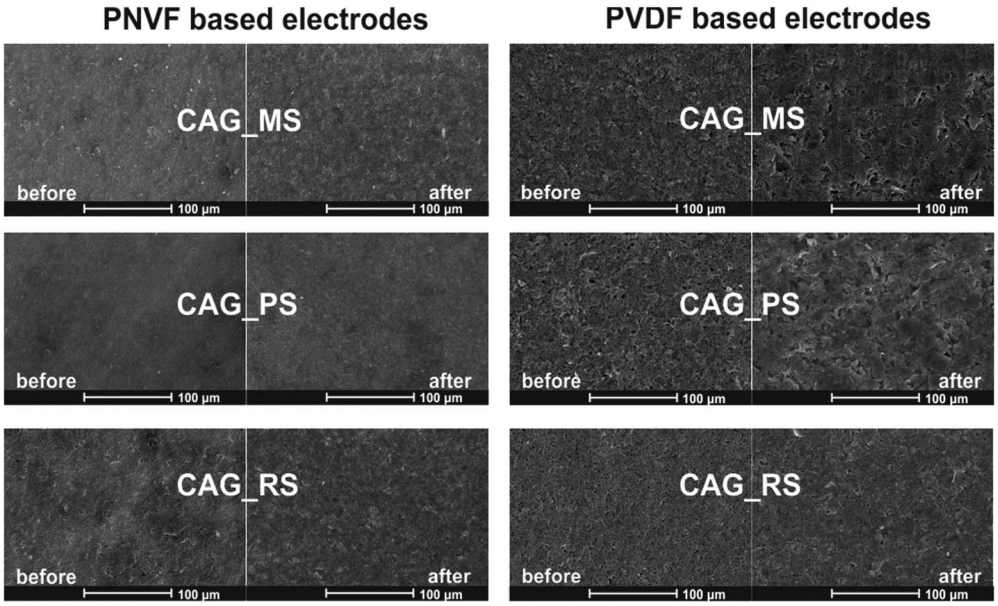

Figure 6. Scanning electron microscopy images of the CAG based electrodes (with different binders) before and after long-term cycling.

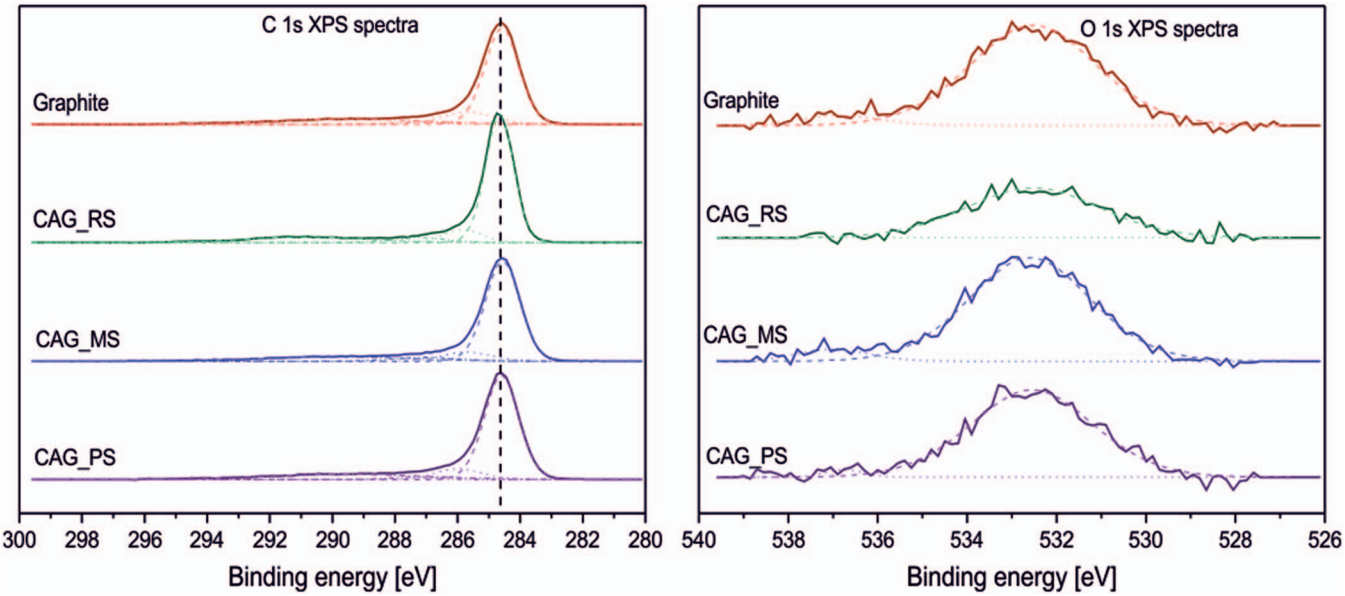

Figure 7. a) The C1s and b) O1s X-ray photoelectron spectra of investigated carbonaceous materials.

active particles and binder) is accompanied by capacity reduction and deterioration of electrode properties. Unlike the electrodes with PVDF, the hydrogen bonds in electrodes with PNVF keep particles together during electrochemical operation. This may be also associated with different morphology of binders that affects the type of created polymeric films (PNVF one seems to be more dense and well-bonded). In fact, the capacity retention when PNVF was applied after 400 cycles at 5C rate in relation to the 101st cycle charge capacity are equal to 100% for Li/Li$^+$/CAG_PS, Li/Li$^+$/CAG_MS and Li/Li$^+$/CAG_RS and over 100% for Li/Li$^+$/graphite due to the constantly raising capacity during conducted experiment. By contrast, the capacity retention values for the carbonaceous electrodes containing PVDF as binder material are equal to 99%, 95%, 84%, 98% for Li/Li$^+$/CAG_PS, Li/Li$^+$/CAG_MS, Li/Li$^+$/CAG_RS and Li/Li$^+$/graphite, respectively.

Furthermore, the amount and the distribution of binders also depend on the morphology of active materials as well as the chemical interaction between these two components. The more functional groups are accessible on the active material surface, the more interacting sites with PNVF are generated. Therefore, creating hydrogen bonds is connected with more homogenous distribution of binder on the surface. Lack of uniformly dispersed polymer leads to the uneven use of anode material grains that can also have unequal topological potential. This phenomenon causes that some of the grains can degrade faster than others as a result of overcharging/overdischarging processes. It affects the cycle life of the electrodes and their capacity fading. We hypothesize that due to the difference in textural properties and less amount of micropores in the CAG_PS structure, this material can have the higher concentration of effectively available functional groups on the surface. These groups are capable of forming hydrogen bonds with PNVF binder what facilitate more homogenous distribution of the polymer in comparison to the rest of the samples. The more uniform distribution could be also responsible for the better transport of Li$^+$ in Li/Li$^+$/CAG_PS cell. However some questions still remain unclear and need to be resolved during further research.

Conclusions

To sum up, poly-N-vinylformamide was explored as a new potential binder for selected anode materials (bio-derived carbon aerogels and graphite). PNVF is an amorphous, water-based polymer, thermally and electrochemically stable, eco-friendly and relatively inexpensive in comparison to PVDF/NMP system. PNVF found to be an efficient binder for carbon aerogels derived from potato starch and the enhancement of electrochemical performances should be attributed to the unique morphology of this carbonaceous material. However we hypothesize that PNVF could also be a promising binder for other anode materials depending on their morphological properties.

In addition, the results show that binder plays a crucial role in the electrode designing process because it importantly affects its electrochemical behavior. By improving physicochemical properties of the electrode such as adhesion strength or binder distribution we can also accomplish the rate capability and the specific capacity of the Li-ion cell. As it can be seen the mechanical properties of the electrode are one of the key factors to obtain its satisfying performance and efficiency. Therefore, the proper selection of binder for every active material is the significant issue that cannot be neglected.

Acknowledgments

This work was financially supported by the National Science Centre – Poland, under research grant no. 2015/19/B/ST8/01077.

ORCID

Marcin Molenda https://orcid.org/0000-0001-6566-7103

References

1. C. Pillot, The Rechargeable Battery Market and Main Trends 2016–2025, Presentation at 33rd Annual International Battery Seminar & Exhibit, 20 March 2017, Fort Lauderdale, FL, USA (accessed: October 2018).
2. Y. Shi, X. Zhou, and G. Yu, *Acc. Chem. Res.*, **50**, 2642 (2017).
3. L. Monconduit, L. Croguennec, and R. Dedryvére, *Electrodes for Li-ion Batteries Materials, Mechanisms and Performance*, ISTE & Wiley, London (2015).
4. M. Müller, L. Pfaffmann, S. Jaiser, M. Baunach, V. Trouillet, F. Scheiba, P. Scharfer, W. Schabel, and W. Bauer, *J. Power Sources*, **340**, 1 (2017).
5. R. J. Brodd and K. Tagawa, in *Advances in Lithium-ion batteries*, V. A. van Schalkwijk and B. Scrosati, Editors, p. 267, Kluwer Academic Publishers, New York (2002).
6. S. Chou, Y. Pan, J. Wang, H. Liu, and S. Dou, *Phys. Chem. Chem. Phys.*, **16**, 20347 (2014).
7. A. Nagai, in *Lithium-ion batteries. Science and Technologies*, M. Yoshio, R.J. Brodd, and A. Kozawa, Editors, p. 155, Springer, New York (2009).
8. G. Liu, H. Zheng, X. Song, and V. S. Battaglia, *J. Electrochem. Soc.*, **159**, A214 (2012).
9. H. K. Park, B. S. Kong, and E. S. Oh, *Electrochem. Commun.*, **13**, 1051 (2011).
10. J. Chen, J. Liu, Y. Qi, T. Sun, and X. Li, *J. Electrochem. Soc.*, **160**, A1502 (2013).
11. B. Lestriez, *Comptes Rendus Chim.* **13**, 1341 (2010).
12. J. Li, Z. Y. Wu, Y. Q. Lu, Y. Zhou, Q. A. Huang, L. Huang, and S. G. Sun, *Adv. Energy Mater.*, **7**(24), 1701185 (2017).

13. S. F. Lux, F. Schappacher, A. Balducci, S. Passerini, and M. Winter, *J. Electrochem. Soc.*, **157**(3), A320 (2010).
14. B. John and G. Cheruvally, *Polym. Adv. Technol.*, **28**(12), 1528 (2017).
15. Z. Zhang, T. Zeng, Y. Lai, M. Jia, and J. Li, *J. Power Sources*, **247**, 1 (2014).
16. H. Zhong, J. He, and L. Zhang, *Mater. Res. Bull.*, **93**, 194 (2017).
17. S. Komaba, K. Shimomura, N. Yabuuchi, T. Ozeki, H. Yui, and K. Konno, *J. Phys. Chem. C*, **115**, 13487 (2011).
18. D. Shin, H. Park, and U. Paik, *Electrochem. Commun.*, **77**, 103 (2017).
19. J. Chong, S. Xun, H. Zheng, X. Song, G. Liu, P. Ridgway, and V. S Battaglia, *J. Power Sources*, **196**(18), 7707 (2011).
20. Z. Zhang, T. Zeng, C. Qu, H. Lu, M. Jia, Y. Lai, and J. Li, *Electrochim. Acta*, **80**, 440 (2012).
21. L. Gong, M. H. T. Nguyen, and E. S. Oh, *Electrochem. Commun.*, **29**, 45 (2013).
22. H. Sheng-Shu, S. Bing-Xuan, and T. Hsisheng, *Electrochemical Study of Poly(N-vinylformamide) as a Binder for $LiFePO_4$ in Li-Ion Batteries*, presented as a poster during the 19th International Meeting on Lithium Batteries (IMLB 2018), Kyoto, Japan, 17th-22nd June 2018.
23. M. Bakierska, M. Molenda, D. Majda, and R. Dziembaj, *Procedia Eng*. **98**, 14 (2014)
24. M. Bakierska, M. Molenda, A. Chojnacka, and M. Świętosławski, WO2017153855A1, 2017.
25. M. Bakierska, A. Chojnacka, M. Świętosławski, P. Natkański, M. Gajewska, M. Rutkowska, and M. Molenda, *Mater*. **10**(11), 1336 (2017).
26. M. Molenda, R. Dziembaj, M. Drozdek, E. Podstawka, and L. M. Proniewicz, *Solid State Ion*. **179**(1–6), 197 (2008).